

# New Hydrotalcite-like Compounds Containing Yttrium

J. M. Fernández,<sup>†</sup> C. Barriga,<sup>†</sup> M. A. Ulibarri,<sup>\*,†</sup> F. M. Labajos,<sup>‡</sup> and V. Rives<sup>‡</sup>

*Dpto. de Química Inorgánica e Ingeniería Química, Facultad de Ciencias,  
Universidad de Córdoba, 14004-Córdoba, Spain, and Dpto. de Química Inorgánica,  
Universidad de Salamanca, 37008-Salamanca, Spain*

*Received July 16, 1996. Revised Manuscript Received September 26, 1996*

Layered double hydroxides (LDHs) containing  $\text{Mg}^{2+}$ ,  $\text{Al}^{3+}$ , and  $\text{Y}^{3+}$  in the brucite-like layers and with carbonate as counteranion have been prepared following the coprecipitation method at constant pH. The Al/Y ratio depends on the concentrations in the starting solutions. The crystallinity of the layered materials decreases as the Al/Y ratio increases, probably due to the distortions introduced by the large difference in the ionic radii of the cations. On calcination at 750 °C MgO (probably containing  $\text{Al}^{3+}$  cations) and  $\text{Y}_2\text{O}_3$  are formed from the sample richest in Y, while the other samples lead to formation of MgO and presumably  $\text{Al}_2\text{Y}_4\text{O}_9$ . At 1000 °C, MgO,  $\text{MgAl}_2\text{O}_4$ , and  $\text{Al}_2\text{Y}_4\text{O}_9$  are formed in all cases. Exposure of samples calcined at 750 °C in air at room temperature leads to reconstruction of a Mg,Al hydrotalcite and segregation of Y-containing phases.

## Introduction

Layered double hydroxides (LDHs) constitute a class of layered compounds complementary to classic clays, as they contain positively charged layers and anions in the interlamellar space. The so-called "hydrotalcite-like compounds" are LDHs with the general formula  $[\text{M}_{1-x}\text{M}_x^{III}(\text{OH})_2]^{x+}\text{A}_x^{z-}\cdot n\text{H}_2\text{O}$ , displaying the  $\text{CdI}_2$  structure with a partial isomorphous  $\text{M}^{II}/\text{M}^{III}$  substitution, the corresponding positive charge being balanced by interlayer anions. Water molecules also exist between the layers.<sup>1–3</sup>

Many papers deal with the composition and structures of these materials, where divalent (Mg, Zn, Ni, ...) and trivalent (Al, Fe, Cr, ...) cations exist;<sup>4,5</sup> only a few systems have been described containing two divalent cations and aluminum, despite their interest as precursors for mixed oxides catalysts (i.e., CuO/ZnO/ $\text{Al}_2\text{O}_3$ ).<sup>4,6,7</sup> Very few systems containing one divalent and two different trivalent cations have been described.<sup>8,9</sup> In the present paper, we report on a new LDH possessing the hydrotalcite-like structure containing Mg, Al, and Y in the hydroxide layer as a potential precursor to mixed oxides currently prepared by ceramic methods.<sup>10</sup> Yttrium aluminum garnets used as hard

gemstones, and sometimes containing other cations, also have interesting magnetic properties.<sup>11</sup>

The synthesis was carried out by coprecipitation of Mg(II), Al(III), and Y(III) cations at 60 °C with strongly alkaline solutions. The changes induced by thermal treatment have also been studied. Finally, the nature of mixed oxides obtained by calcination at increasing temperatures has been assessed by X-ray diffraction.

## Experimental Section

**Synthesis of the Samples.** Three samples have been prepared. They differ in the Al/Y atomic ratio and are named accordingly. Synthesis of sample A4Y1 was carried out at 60 °C by dropwise addition of 100 mL of a solution containing  $\text{Mg}(\text{NO}_3)_2\cdot 6\text{H}_2\text{O}$  (0.3 M),  $\text{Y}(\text{NO}_3)_3\cdot \text{aq}$  (ca. 0.02 M), and  $\text{Al}(\text{NO}_3)_3\cdot 9\text{H}_2\text{O}$  (0.08 M) to 100 mL of a 0.1 M  $\text{Na}_2\text{CO}_3$  solution (pH = 11.47); for samples A2Y1 and A1Y1 the  $\text{Al}^{3+}$  and  $\text{Y}^{3+}$  nitrate concentrations were 0.066 and 0.033 M, and 0.05 and 0.05 M, respectively. When naming the samples, the figures stand for the integer closest to the  $\text{Al}^{3+}/\text{Y}^{3+}$  atomic ratio. In this way, we tried to prepare solids with an atomic ratio  $\text{M}^{2+}/\text{M}^{3+}$  (i.e., divalent to trivalent cations in the layers) of 3.00 but with an  $\text{Al}^{3+}/\text{Y}^{3+}$  ratio of 4, 2, and 1, respectively. Regardless of this ratio, a white precipitate is immediately formed upon addition of the first drop of the mixed-metal nitrate solution to the basic  $\text{Na}_2\text{CO}_3$  solution. Once the pH of the reaction mixture reached a value close to 10.0, a 0.1 M NaOH solution was added along with the mixed  $\text{Mg}^{2+}/\text{Al}^{3+}/\text{Y}^{3+}$  solution to hold the reaction pH at a value of 10.0. After complete addition of the mixed nitrate solution (ca. 3 h from start), the reaction mixture was aged while magnetically stirred for 8 h, with the pH maintained at a value of 10 using 0.1 M NaOH and a Metrohm Dosimat 725 apparatus. The white product was centrifuged and washed several times with distilled, deionized water, until no infrared bands due to nitrate were detected. The solid was finally dried in an open-air oven at 60 °C.

**Characterization.** Mg, Al, and Y contents were determined by ICP at Servicio General de Análisis Químico Aplicado (University of Salamanca, Spain) and also by EDAX, in a Philips PSEM 500 microscope coupled to an electronic microprobe (detection unit ECON IV). Elemental chemical analysis

<sup>†</sup> Universidad de Córdoba.

<sup>‡</sup> Universidad de Salamanca.

\* To whom all the correspondence should be sent. E-mail: iq1ulcom@uco.es

- (1) Allmann, R. *Acta Crystallogr. Sect. B* **1986**, 24, 972.
- (2) Taylor, H. F. W. *Mineral. Mag.* **1973**, 39, 377.
- (3) Miyata, S. *Clays Clay Miner.* **1975**, 23, 369.
- (4) Cavani, F.; Trifirò, F.; Vaccari, A. *Catal. Today* **1991**, 11, 173.
- (5) de Roy, A.; Forano, C.; El-Malki, K.; Besse, J. P. In *Synthesis of Microporous Materials*; Ocelli, M. L.; Robson, M. E., Eds.; Van Nostrand Reinhold: New York, 1992; Vol. II, p 108.
- (6) Kooli, F.; Kosuge, K.; Tsunashima, A. *J. Mater. Sci.* **1995**, 30, 4591.
- (7) Kooli, F.; Kosuge, K.; Hibino, T.; Tsunashima, A. *J. Mater. Sci.* **1993**, 28, 2769.
- (8) Kooli, F.; Kosuge, K.; Tsunashima, A. *J. Solid. State Chem.* **1995**, 118, 285.
- (9) Barriga, C.; Kooli, F.; Rives, V.; Ulibarri, M. A. In *Synthesis of Porous Materials: Zeolites, Clays and Nanostructures*; Ocelli, M. L.; Kessler, H., Eds.; Marcel Dekker: New York, 1996; Chapter 41, p 661.
- (10) Joint Committee on Powder Diffraction Standard—International Centre for Diffraction Data, Swarthmore, PA, 1988, file 34-368.

(11) Weast, R. C., Ed. *Handbook of Chemistry and Physics*, 57th ed.; CRC Press: Cleveland, 1973; p B-58.

**Table 1. Metal Contents Data and Specific Surface Areas for A4Y1, A2Y1, and A1Y1 Samples**

sample	A1Y1	A2Y1	A4Y1
Mg <sup>a</sup>	17.1	19.7	16.2
Al <sup>a</sup>	3.8	5.2	5.2
Y <sup>a</sup>	10.1	4.0	2.6
M <sup>2+</sup> /M <sup>3+</sup>	2.8 (3.0)	3.4 (3.8)	2.8 (3.2)
Al <sup>3+</sup> /Y <sup>3+</sup>	1.3 (1.3)	3.8 (3.8)	7.0 (8.5)
SBET <sup>c</sup>	47	50	46

<sup>a</sup> % weight, as determined by ICP. <sup>b</sup> Atomic ratio by ICP (values determined by EDAX in brackets). <sup>c</sup> Specific surface area, m<sup>2</sup> g<sup>-1</sup>.

using spectrophotometric methods were discarded due to the strong interferences between Al and Y.<sup>12</sup>

Powder X-ray diffraction (PXRD) diagrams were obtained with a Siemens D500 instrument, using Cu K $\alpha$  radiation (graphite monochromator) at a scanning speed of 2°(2 $\theta$ )/min.

Transmission electron micrographs (TEM) were obtained in a JEOL 200CX microscope. Samples were dispersed in acetone by ultrasound and settled on copper grids covered with a carbon film for examination.

The Fourier transform infrared spectra (FT-IR) of the samples were recorded in a Perkin-Elmer FT-IR 1730 apparatus, with a nominal resolution of 2 cm<sup>-1</sup> and averaging 100 scans; the sample was pressed in KBr pellets (concentration ca. 3 mg of sample/100 mg of KBr).

Differential thermal analysis (DTA) and thermogravimetric analysis (TG) were performed on Perkin-Elmer DTA 1700 and TGS-2 instruments, respectively, using flowing air (60 mL min<sup>-1</sup>) at a heating rate of 12 °C min<sup>-1</sup>.

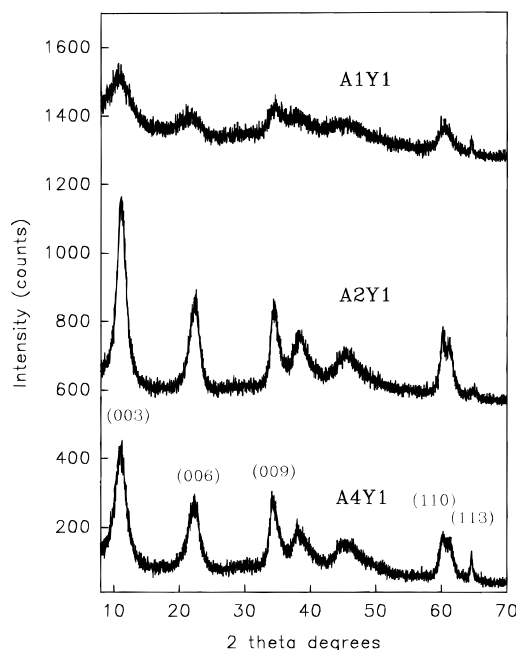
Specific surface areas of the samples were measured by the single-point method using a Micromeritics Flowsorb II 2300 instrument, using a N<sub>2</sub>/He (30/70) gas mixture from Sociedad Española del Oxígeno (SEO, Spain).

## Results and Discussion

**Hydrotalcite-like Materials.** Elemental chemical analysis results for the three samples are given in Table 1. It should be noted that both the M<sup>2+</sup>/M<sup>3+</sup> and the Al<sup>3+</sup>/Y<sup>3+</sup> ratios calculated using ICP and EDAX are slightly different. So, while the expected value for ratio M<sup>2+</sup>/M<sup>3+</sup> would be 3.00, values obtained are in the range 2.79–3.38 (as determined by ICP) or 3.02–3.80 (as determined by EDAX). The values obtained by IPC are 2.99  $\pm$  13% (values from EDAX are merely indicative and cannot be taken as quantitative).

The Al<sup>3+</sup>/Y<sup>3+</sup> ratios results were markedly different from those used in the starting solutions. Sample A1Y1 (expected Al<sup>3+</sup>/Y<sup>3+</sup> = 1) had a value of 1.27 using both methods, sample A2Y1 (expected Al<sup>3+</sup>/Y<sup>3+</sup> = 2) was 3.80 and, finally, for sample A4Y1 (expected Al<sup>3+</sup>/Y<sup>3+</sup> = 4) it was 7.00 (ICP) or 8.45 (EDAX). In other words, the solid is enriched in aluminum when compared with the composition of the starting nitrate solutions. This indicates that a complete precipitation of yttrium is difficult and that this is more evident as the Al<sup>3+</sup>/Y<sup>3+</sup> ratio is increased.

Powder X-ray diffraction patterns of three samples are shown in Figure 1. First of all, the low crystallinity of sample A1Y1 is noted. The overall aspect of the diagrams indicates a layered structure, peaks due to basal diffractions being observed at 8.09, 4.02, and 2.60 Å for sample A1Y1 and at 8.02, 3.98, and 2.60 Å for both samples A2Y1 and A4Y1. For a layered, hydrotalcite-like material, these three peaks correspond to diffraction

**Figure 1.** PXRD diagrams of untreated A1Y1, A2Y1, and A4Y1 samples.

by planes (003), (006), and (009), respectively.<sup>3,13,14</sup> The value for the (003) peak at 8.09–8.03 Å is significantly larger than the value reported for natural hydrotalcite, 7.68 Å.<sup>15</sup> This value is related to the thickness of the brucite-like layers (4.8 Å for hydrotalcite<sup>1</sup>), as well as to the size of the anion (and, in some cases, its orientation) and the number of water molecules existing in the interlayer.<sup>16,17</sup> However, the hydration degree in the interlayer is almost the same in our samples and in natural hydrotalcite (see below), and in all cases the interlayer anion is the same (carbonate). Therefore the increase may be related to the increase in the thickness of the brucite-like layers, due to the aluminum/yttrium substitution. The ionic radii reported<sup>18</sup> for octahedrally coordinated Al<sup>3+</sup> and Y<sup>3+</sup> are 0.675 and 1.04 Å, respectively. A similar variation has been observed in other hydrotalcite-like compounds upon substitution of cations in the layers with markedly different ionic radii.<sup>9</sup> In addition, the slight increase in basal spacing with increasing yttrium content is consistent with the lower polarizing ability of Y<sup>3+</sup> (if compared to Al<sup>3+</sup>), then decreasing the Coulombic attractive force between the positively charged brucite-like layers and the negatively charged interlayer anions.<sup>19</sup> The markedly low crystallinity of sample A1Y1 could be also related to the relatively large yttrium content in this sample, thus introducing large distortions in the layers, because of the different ionic radii (Mg<sup>2+</sup> in octahedral coordination 0.86 Å, values for octahedrally coordinated Al<sup>3+</sup> and Y<sup>3+</sup> given above).

The other PXRD feature characteristic of the hydrotalcite structure is the doublet recorded between 60 and

(13) Bish, D. L. *Bull. Mineral.* **1980**, *103*, 170.

(14) Hansen, H. C. B.; Taylor, R. M. *Clay Miner.* **1991**, *26*, 507.

(15) Joint Committee on Powder Diffraction Standard—International Centre for Diffraction Data, Swarthmore, PA, 1988, file 14-191.

(16) Kruissink, E. C.; von Reijen, L. L.; Ross, J. R. H. *J. Chem. Soc., Faraday Trans. 1* **1981**, *77*, 649.

(17) Yun, S. K.; Pinnavaia, T. J. *Chem. Mater.* **1995**, *7*, 348.

(18) Huheey, J. E.; Keiter, E. A.; Keiter, R. L. *Inorganic Chemistry. Principles of Structure and Reactivity*, 4th ed.; Harper Collins: New York, 1993.

(19) Brindley, G. W.; Kikkawa, S. *Am. Miner.* **1979**, *64*, 836.

(12) Burriel, F.; Lucena, F.; Arriba, S.; Hernández, J. *Química Analítica Cualitativa*, 13th ed.; Paraninfo: Madrid, 1989.

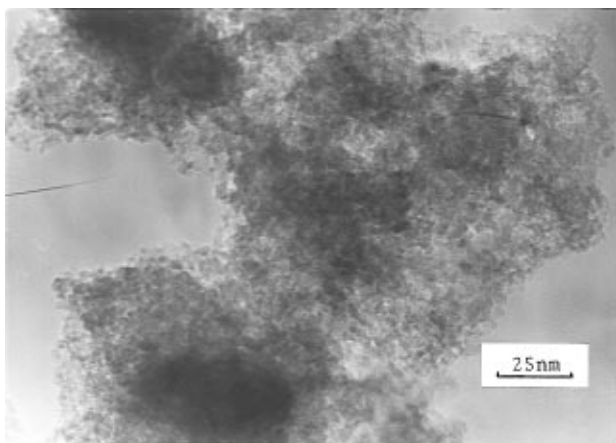


Figure 2. TEM of sample A2Y1.

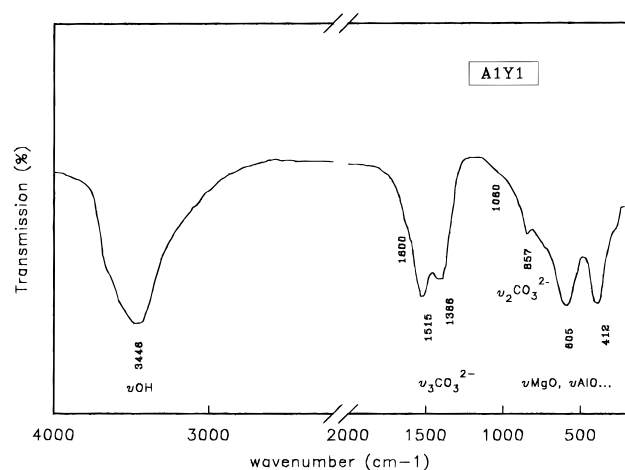


Figure 3. FT-IR spectrum of sample A1Y1.

65°(2 $\theta$ ). These maxima are due to diffraction by planes (110) and (113). The lattice parameter  $a$  is related to the (110) spacing according to  $a = 2d(110)$ .<sup>4</sup> Unfortunately, the very low crystallinity of sample A1Y1 makes it a highly imprecise determination of the positions of these maxima; moreover, they are recorded as a single peak at 1.53 Å. The (110) and (113) peaks are recorded at 1.54 and 1.51 Å, respectively, for samples A2Y1 and A4Y1. Although incorporation of Y<sup>3+</sup> gives rise to an increase in the value of  $c$  (see above), such an incorporation does not necessarily give rise to a similar increase in  $a$ : it should be noted that  $c$  corresponds to 3 times the distance *between* the brucite-like layers, whereas dimension  $a$  is measured *within* the layers. Once any amount of Y<sup>3+</sup> enters into the layer,  $c$  should increase, but without changing appreciably as more and more yttrium is present in the layer. A large increase in  $a$  would, however, require large amounts of yttrium.

The TEM micrographs of the three samples show similar agglomerates of small particles (Figure 2), in agreement with the similar values (almost coincident, within experimental error) for the specific surface areas of the samples (Table 1).

The FT-IR spectra for samples Mg–Al–Y were very similar, sample A1Y1 is shown in Figure 3. The broad band at ca. 3446 cm<sup>−1</sup> is due to the stretching mode of hydroxyl groups, both from those existing in the brucite-like layers and from the water molecules existing in the interlayer space. The bending mode band of water molecules, usually recorded close to 1600 cm<sup>−1</sup>, is

recorded only as a weak shoulder on the large wavenumbers side of the strong band at 1515 cm<sup>−1</sup>. This band, together with its companion one at 1388 cm<sup>−1</sup>, should be due to mode  $\nu_3$  of interlayer carbonate species. This band is recorded at 1450 cm<sup>−1</sup> for free carbonate species ( $D_{3h}$  symmetry) but splits and shifts upon a symmetry lowering. So, for calcite (local symmetry around the carbonate anion  $D_3$ ) it has been reported in the range 1492–1429 cm<sup>−1</sup>, while for aragonite (local symmetry  $C_s$ ) it splits into two bands at 1504 and 1492 cm<sup>−1</sup>.<sup>20</sup> In the present case, the splitting is even larger, probably due to the restricted symmetry in the interlayer space, in addition to the different electrostatic interactions because of the distortions originated by the three, very-different sized cations in the layers. Such a large splitting (ca. 115 cm<sup>−1</sup>) has been previously reported for carbonate species formed upon adsorption of CO<sub>2</sub> on aluminum hydroxide gel.<sup>21</sup> The band at 857 cm<sup>−1</sup> is due to mode  $\nu_2$  of carbonate (879 cm<sup>−1</sup> for free ion and calcite, 866 cm<sup>−1</sup> for aragonite). Lower wavenumber bands at 605 and 412 cm<sup>−1</sup> are due to lattice vibrations (Mg–O, Al–O, Y–O, Mg–O–Al, ...),<sup>22</sup> while mode  $\nu_4$  of carbonate could be responsible for the weak shoulder close to 724 cm<sup>−1</sup> (706 cm<sup>−1</sup> for free carbonate and calcite, split into two bands at 711 and 706 cm<sup>−1</sup> for aragonite). Activation of mode  $\nu_1$  (originally forbidden in IR for a  $D_{3h}$  symmetry) has been observed in some cases,<sup>21,23,24</sup> and could account for the weak shoulder at 1060 cm<sup>−1</sup> (1080 cm<sup>−1</sup> for aragonite and 1060 cm<sup>−1</sup> for CO<sub>2</sub> adsorbed on aluminum hydroxide gel).<sup>21</sup> Nevertheless, the positions of the bands originated by modes  $\nu_1$  and  $\nu_4$  are only tentative, due to the difficulty in locating precisely their positions on the sides of much stronger bands.

The DTA profiles for three samples are shown in Figure 4. All profiles show two strong endothermic peaks within 140–180 °C (due to dehydration)<sup>25–28</sup> and 370–400 °C (dehydroxylation and decarbonation).<sup>25–28</sup> The traces are slightly different in the precise position and relative intensities of the peaks. The larger intensity of the first endothermic peak for sample A4Y1 is in agreement with the larger water content for this sample, as concluded from TG analysis (see below). The second peak moves slightly toward lower temperatures as the Y content is decreased, while the first peak shifts in the opposite direction. For Mg,Al hydrotalcite, the first endothermic peak is recorded at 270 °C;<sup>29,30</sup> in our case it is recorded at 143 °C for sample A1Y1, at 170 °C for A2Y1, and the average temperature value for the two peaks recorded for sample A4Y1 is at 175 °C. These results are not unexpected, as the sample whose chemi-

(20) Nakamoto, K. *Infrared and Raman spectra of Inorganic and Coordination Compounds*, 4th ed.; Wiley: New York, 1986.

(21) Serna, C. J.; White, J. L.; Hem, S. L. *Soil Sci. Soc. Am. J.* **1977**, *41*, 1009.

(22) Hernández-Moreno, M. J.; Ulibarri, M. A.; Rendón, J. L.; Serna, C. J. *Phys. Chem. Miner.* **1985**, *12*, 34.

(23) Barriga, C.; Fernández, J. M.; Ulibarri, M. A.; Labajos, F. M.; Rives V. J. *Solid. State Chem.* **1996**, *124*, 205.

(24) Labajos, F. M.; Rives V.; Ulibarri, M. A. *Spectrosc. Lett.* **1991**, *24*, 499.

(25) Miyata, S. *Clays Clay Miner.* **1983**, *31*, 305.

(26) Brindley, G. W.; Kikkawa, S. *Clays Clay Miner.* **1980**, *28*, 87.

(27) Hernández, M. J.; Ulibarri, M. A.; Rendón, J. L.; Serna, C. J. *Thermochim. Acta* **1984**, *81*, 311.

(28) Fernández, J. M.; Barriga, C.; Ulibarri, M. A.; Labajos, F. M.; Rives, V. J. *Mater. Chem.* **1994**, *4*, 1117.

(29) Marino, O.; Mascolo, G. In *Proc. 2nd. European Symp. Thermal Analysis*; Dollimore, D., Ed.; Heyden: London, 1981; p 391.

(30) Ross, G. I.; Kodama, H. *Am. Miner.* **1967**, *52*, 1037.

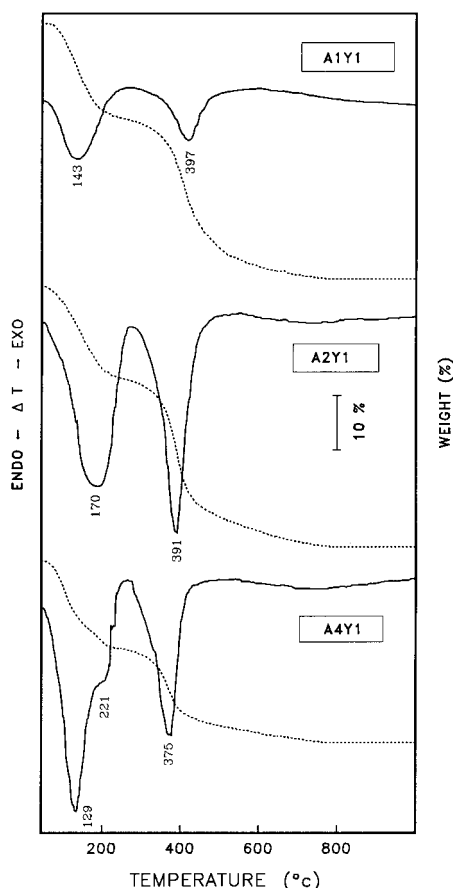


**Figure 4.** TG (dotted lines) and DTA (solid lines) profiles of the A1Y1, A2Y1, and A4Y1 samples.

cal composition is closer to that of pure hydrotalcite (A4Y1) shows the first endothermic peak at the highest temperature. It should be also noted that peaks for samples A1Y1 and A2Y1 are rather broad. We can tentatively argue that in all three cases two endothermic processes should be included, but splitting is observed only for sample A4Y1. The marked asymmetry in the first peak here recorded is probably due to a heterogeneous distribution of water molecules, i.e., water molecules should be held with a different strength in the interlayer space. Also the second peak shows a prominent shoulder at low temperatures. As the  $Y^{3+}$  content increases, molecular water is removed at lower temperature, in agreement with the lower charge-to-size ratio for  $Y^{3+}$  than for  $Al^{3+}$ .

The TG traces are also included in Figure 4. Two weight losses are recorded, coinciding with the endothermic peaks in the DTA profiles. As expected, the first weight loss for sample A4Y1 can be tentatively resolved in two overlapped processes. The outline of both DTA and TG curves are very similar to those previously reported by several authors for hydrotalcite-like materials,<sup>31</sup> thus suggesting that a single phase exists, as no additional DTA peak or TG loss are recorded. However, weight losses and DTA minima are recorded at lower temperatures than for hydrotalcite, suggesting that the presence of  $Y^{3+}$  in the lattice somewhat favors water removal.

Total weight loss after calcination at 800 °C corresponds to ca. 50% of the initial sample weight. From

**Table 2.** Chemical Formulas of the Mg,Al,Y Hydrotalcite-like Compounds Prepared<sup>a</sup>

sample	$\Delta W^b$	formula
A1Y1	48	$[Mg_{0.74}Al_{0.15}Y_{0.11}(OH)_2](CO_3)_{0.13} \cdot 0.87H_2O$
A2Y1	46	$[Mg_{0.77}Al_{0.18}Y_{0.05}(OH)_2](CO_3)_{0.11} \cdot 0.74H_2O$
A4Y1	50	$[Mg_{0.74}Al_{0.23}Y_{0.03}(OH)_2](CO_3)_{0.13} \cdot 1.19H_2O$

<sup>a</sup> Figures have been rounded to two digits. <sup>b</sup> Total weight loss (%) after calcination at 800 °C.

the weight losses recorded up to the first plateau (ca. 245 °C) and the chemical composition of the samples (see Table 1) and assuming that carbonate is the only anion in the interlayer space (in agreement with FT-IR data above), the amount of water molecules existing in the interlayer space, and hence, the formulas of the compounds, can be determined. The results are given in Table 2.

**Calcined Products.** The nature of the crystalline phases existing in the samples after calcination at increasing temperatures are of interest. We have chosen calcination temperatures from information provided by the DTA results. The samples were calcined at 245 °C (after dehydration), 450 °C (immediately after dehydroxylation/decarbonation), and at 700 and 1000 °C, where well-crystallized phases are expected to be formed. Samples will be named A1Y1/T or A2Y1/T or A4Y1/T, where T stands for the calcination temperature, in °C. The corresponding PXRD patterns are included in Figures 5–7. The layered structure seems to be stable up to 245 °C for samples A2Y1 and A4Y1. The poor crystallinity observed for the uncalcined sample A1Y1 (Figure 1) results in a very weak pattern after calcination at 245 °C. For the other two samples, however, typical patterns of hydrotalcite-like material are obtained, although the (00*l*) diffraction lines are shifted toward lower spacing values, due to removal of interlayer water molecules removal.

After calcination at 550 °C (i.e., after removal of hydroxyl groups from the brucite-like layers, and carbonate anions, as carbon dioxide, from the interlayer), the layered structure collapses, and only two peaks are recorded at 2.106 and 1.489 Å, corresponding to planes (200) and (220) of MgO, respectively. However, these peaks are very broad. Sato et al.<sup>32</sup> have reported that thermal decomposition of Mg,Al hydrotalcite at 420 °C gives rise to formation of magnesium aluminum oxide, that decomposes above 1000 °C to MgO and  $MgAl_2O_4$ . Such a process leads to a decrease in the value of the lattice constant as the  $Al^{3+}$  content increases, mainly due to the lower ionic size of  $Al^{3+}$  than  $Mg^{2+}$ . In the present case, such a change in lattice constant *a* for the rock-salt structure of Mg,Al oxide is difficult to check for sample A1Y1, as the ionic size of  $Mg^{2+}$  is larger than that of  $Al^{3+}$  but smaller than that of  $Y^{3+}$ . However, the analysis of results for sample A4Y1 (where a very large excess of  $Al^{3+}$  on  $Y^{3+}$  exists) provides some clues on the nature of the solid calcined at 550 °C. The lattice constant *a* for samples A1Y1/550, A2Y1/550, and A4Y1/550 are 4.219, 4.204, and 4.182 Å, respectively (as calculated by fitting the diffraction peaks to Pearson VII functions<sup>33</sup>), while for MgO it is 4.212 Å. That is, the value of *a* decreases as the  $Y^{3+}$  content decreases ( $Al^{3+}$

(31) Sato, T.; Fujita, H.; Endo, T.; Shimada, M. *React. Solids* **1988**, 5, 219.

(32) Sato, T.; Fujita, H.; Endo, T.; Shimada, M. *React. Solids* **1986**, 2, 253.

(33) Hall, M. M.; Veeraraghavan, V. G.; Rubin, H.; Winchell P. G. *J. Appl. Crystallogr.* **1977**, 10, 66.

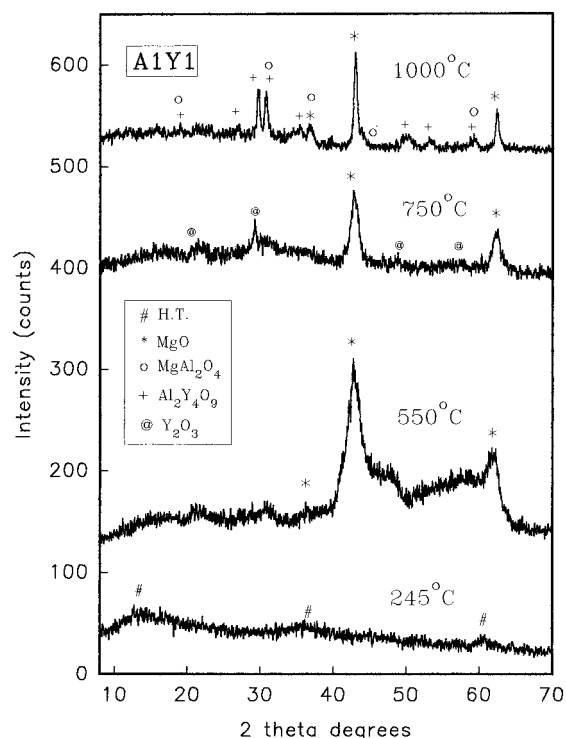


**Figure 5.** PXRD diagrams of sample A1Y1 calcined in air for 2 h at the temperatures given.

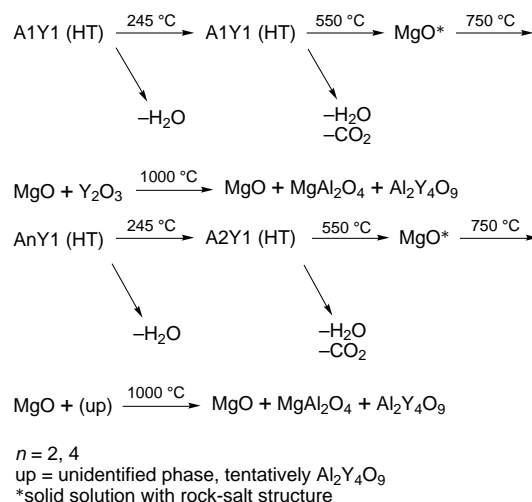
content increases), in agreement with the ionic radii of these cations.

Upon calcination at 750 °C the MgO peaks remain, but additional weak peaks are recorded, ascribed to different crystalline phases depending on the sample. The lattice constant  $a$  for the rock-salt structure changes from the values above given for the samples calcined at 550 °C, approaching the value for pure MgO, in agreement with segregation of  $Y^{3+}$ - and  $Al^{3+}$ -containing phases, identified by PXRD. So, while for sample A1Y1 these peaks are due to  $Y_2O_3$  (Figure 5, main peak at 3.062 Å), for samples A2Y1 and A4Y1 they may be due to  $Al_2Y_4O_9$ . The presence of this compound cannot undoubtedly be ruled out for samples A2Y1 and A4Y1, where a rather low Y concentration exists. The MgO peaks are better defined for samples A2Y1 and A4Y1 than for sample A1Y1.

The TG profiles for these samples show only a small weight loss above 550 °C, but since this weight loss extends over a wide temperature range, no defined effect is recorded in the DTA profiles. On the other hand, no weight loss is recorded above 750 °C. Hibino et al.<sup>34</sup> have recently proposed that the temperature for total decarbonation of Mg,Al hydrotalcite depends on the  $x = Al/(Mg + Al)$  ratio: for  $x = 0.33$  such a decarbonation is only completed after heating at 900 °C, while for  $x = 0.25$  (i.e., the same  $M^{2+}/M^{3+}$  ratio as in our samples),  $CO_2$  evolution is almost complete at 500 °C. So, changes in samples above 500–550 °C should be ascribed solely to crystallization/phase changes.

Calcination at 1000 °C leads to crystallization of well-defined phases. For sample A1Y1, peaks due to  $Y_2O_3$  vanish, and, instead, in addition to MgO peaks, new peaks are recorded due to  $Al_2Y_4O_9$  and to  $MgAl_2O_4$ . A similar behavior is observed for samples A2Y1 and

A4Y1, although in these cases crystallization of  $Al_2Y_4O_9$  was not observed when the samples were calcined at 750 °C. Finally, the intensities of the  $Al_2Y_4O_9$  peaks, relative to those of MgO, are larger for sample A1Y1 than for A4Y1, as expected for the relatively larger yttrium content:



One of the most exploited properties of hydrotalcites is their ability to recover the layered structure after being calcined at temperatures of 400–650 °C, when exposed to air<sup>35,36</sup> or immersed in a solution containing different anions.<sup>37</sup> This property is shown by hydrotalcite-like materials containing a volatile anion, such as carbonate, and the maximum calcination temperature after which recovering of the layered structure is attained depends mainly on the nature of the cations existing in the brucite-like layers.<sup>32,35,36</sup> This behavior can be explained on the basis of the mechanism controlling the thermal decomposition of hydrotalcite-like precursors:<sup>31,38,39</sup> if a layered microstructure is retained after the thermal treatment, recovering of the hydrotalcite-like structure is possible.<sup>31</sup> However, as far as we know, no data have been reported in the literature regarding reconstruction of calcined hydrotalcite-like precursors possessing two different  $M^{2+}$  (or  $M^{3+}$ ) cations in the brucite-like layers. We here report on the behavior shown by the Mg–Al–Y samples.

Usually such a reconstruction is only observed from samples where formation of well-crystallized phases has not been completed (ca. 500 °C in most cases). We have therefore checked reconstruction at room temperature in open air of samples calcined at 750 °C, where only crystalline solid solutions possessing the rock-salt structure have been identified by PXRD (in addition to  $Y_2O_3$  in sample A1Y1 and weak peaks, tentatively ascribed to  $Al_2Y_4O_9$ , for samples A2Y1 and A4Y1).

Reconstruction results for samples A1Y1/750 and A4Y1/750 (i.e., those with the highest and the lowest Y content) are summarized in Figures 8 and 9. First of all, it should be noted that reconstruction takes place, despite the markedly high calcination temperature. As these figures show, reconstruction is clearly attained for

(34) Hibino, T.; Yamashita, Y.; Kosuge, K.; Tsunoshima, A. *Clays Clay Miner.* **1995**, *43*, 427.

(35) Bish, D. L.; Livingstone, A. L. *Miner. Mag.* **1981**, *44*, 339.  
 (36) Moore, P. B. *Lithos* **1971**, *4*, 213.  
 (37) Sato, T.; Wakabayashi, T.; Shimada, M. *Ind. Eng. Chem., Prod. Res. Dev.* **1986**, *25*, 89.  
 (38) Reichle, W. T. *Chemtech* **1986**, *16*, 58.  
 (39) Mascolo, G.; Marino, P. *Thermochim. Acta* **1980**, *35*, 93.

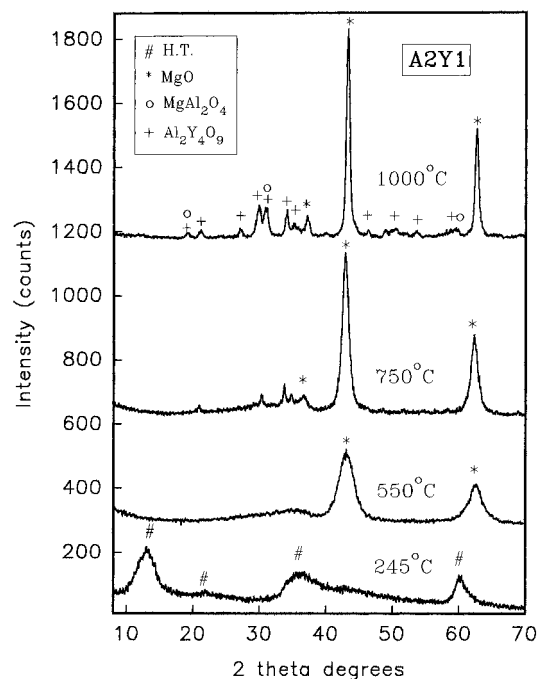


**Figure 6.** PXRD diagrams of sample A2Y1 calcined in air for 2 h at the temperatures given.

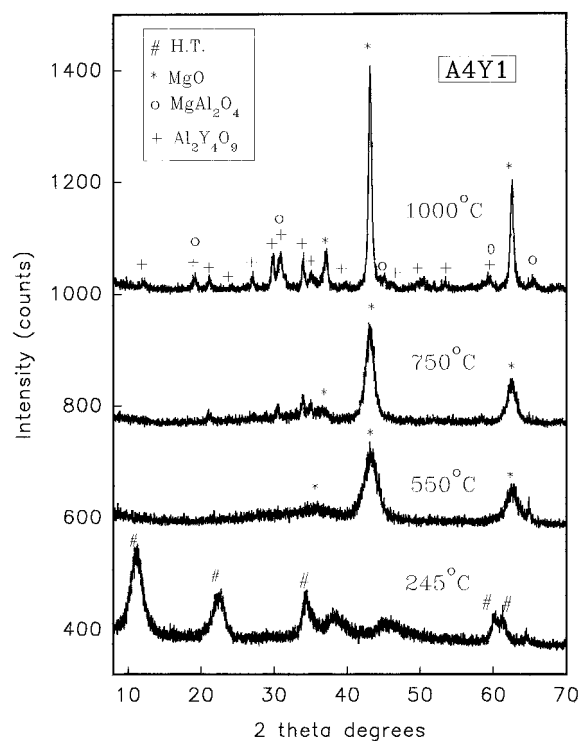


**Figure 7.** PXRD diagrams of sample A4Y1 calcined in air for 2 h at the temperatures given.

sample A4Y1/750, although for sample A1Y1/750 a weak, but distinguishable, peak close to  $7.82 \text{ \AA}$ , due to planes (003) of Mg,Al hydrotalcite,<sup>15</sup> is recorded, together with the more intense diffraction lines due to MgO. For sample A4Y1/750 such a reconstruction process has undoubtedly taken place, with the main diffraction peaks due to a hydrotalcite-like material at  $7.67$ ,  $3.84$ , and  $2.57 \text{ \AA}$ .

Insets in both figures correspond to the  $8^\circ \leq 2\theta \leq 18^\circ$  range, where the diffraction line due to planes (003) is expected. The insets correspond to the PXRD diagrams of the original, uncalcined (hydrotalcite-like material),

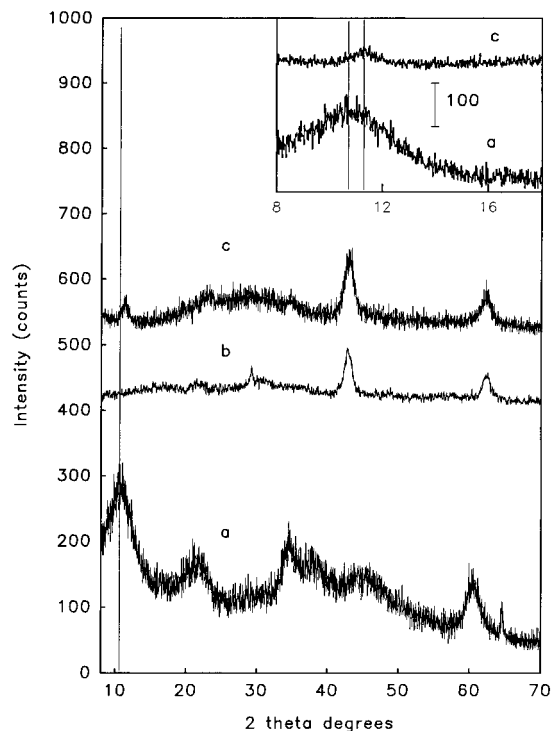


**Figure 8.** PXRD diagrams of sample A1Y1: (a) original, (b) calcined in air  $750^\circ\text{C}$ , (c) calcined in air at  $750^\circ\text{C}$  and exposed to air during 20 days. Inset:  $8\text{--}18^\circ(2\theta)$  range for profiles (a) and (c).

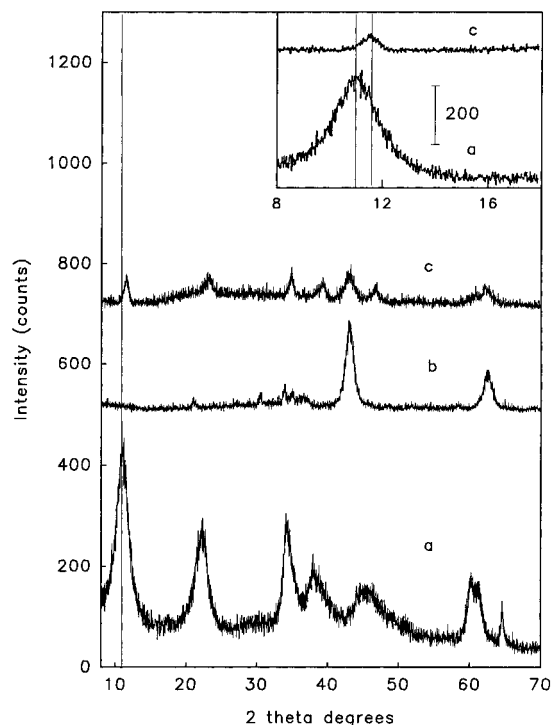


**Figure 9.** PXRD diagrams of sample A4Y1: (a) original, (b) calcined in air  $750^\circ\text{C}$ , (c) calcined in air at  $750^\circ\text{C}$  and exposed to air during 20 days. Inset:  $8\text{--}18^\circ(2\theta)$  range for profiles (a) and (c).

and the reconstructed phase. It is worthwhile to notice that this peak, recorded at  $8.09$  and  $8.03 \text{ \AA}$  for A1Y1 and A4Y1, respectively, shifts to  $7.82$  and  $7.67 \text{ \AA}$  in the reconstructed material. This position is very close to that of Mg,Al hydrotalcite, at  $7.68 \text{ \AA}$ .<sup>15</sup>

The lower extent of reconstruction for sample A1Y1 may be due to the irreversible crystallization of  $\text{Y}_2\text{O}_3$

after calcination at 750 °C. In addition, the fact that the basal spacing coincides with that of the Mg,Al hydrotalcite suggests that segregation takes place, reconstructing the fraction of the solid containing Mg and Al, but leaving appart a phase of  $Y_2O_3$ , probably amorphous, as it was not detected by PXRD.

### Conclusions

When Mg(II), Al(III), and Y(III) are simultaneously precipitated under an air atmosphere from aqueous solutions using NaOH and  $Na_2CO_3(aq)$ , a solid possessing the hydrotalcite-like structure is obtained, with Mg(II), Al(III), and Y(III) ions in the layers. The Al/Y atomic ratio depends on the relative concentrations of the cations in the starting solutions. The Al/Y ratio strongly determines the nature of crystalline phases formed during prolonged calcination of these solids: calcination of A1Y1 at 750 °C leads to formation of MgO and  $Y_2O_3$ , while calcination of A2Y1 and A4Y2 at the same temperature leads to formation of MgO and one unidentified phase (presumably  $Al_2Y_4O_9$ ). However,

calcination at 1000 °C leads to formation of MgO,  $MgAl_2O_4$ , and  $Al_2Y_4O_9$ , regardless of the Al/Y atomic ratio in the starting material. When these materials are exposed to ambient conditions for 20 days, reconstruction of the layered structure is attained. This is accompanied by segregation of Y-containing phases, and reconstruction leads to Mg,Al hydrotalcite.

**Acknowledgment.** The authors thank the financial support of project CICYT (MAT93-787), Junta de Castilla y León (Consejería de Cultura y Turismo) and Junta de Andalucía (Research Group FQM 214). This work is within the Concerted European Action on Pillared Layered Solids (CEA-PLS). The authors also thank Mr. A. Montero for his assistance in obtaining some of the experimental results.

CM9603720

---

© Abstract published in *Advance ACS Abstracts*, December 1, 1996.